Redox Biology 50 (2022) 102252

Contents lists available at ScienceDirect

Redox Biology

journal homepage: www.elsevier.com/locate/redox

Flow-induced endothelial mitochondrial remodeling mitigates mitochondrial reactive oxygen species production and promotes mitochondrial DNA integrity in a p53-dependent manner

Junchul Shin [a,b,1], Soon-Gook Hong [a,1], Soo Young Choi [b], Meghan E. Rath [a], Jason Saredy [b,c], Daniel G. Jovin [b], Jacqueline Sayoc [b], Hye-Sang Park [b], Satoru Eguchi [b], Victor Rizzo [b], Rosario Scalia [b], Hong Wang [c], Steven R. Houser [b], Joon-Young Park [a,b,*]

[a] From the Department of Kinesiology, Temple University, Philadelphia, PA, USA
[b] Cardiovascular Research Center, Temple University, Philadelphia, PA, USA
[c] Center for Metabolic Disease Research, Temple University, Philadelphia, PA, USA

ARTICLE INFO

Keywords:
p53
Fluid shear stress
Mitochondria
Endothelial cell
mtROS
TFAM

ABSTRACT

Tumor suppressor *p53* plays a pivotal role in orchestrating mitochondrial remodeling by regulating their content, fusion/fission processes, and intracellular signaling molecules that are associated with mitophagy and apoptosis pathways. In order to determine a molecular mechanism underlying flow-mediated mitochondrial remodeling in endothelial cells, we examined, herein, the role of *p53* on mitochondrial adaptations to physiological flow and its relevance to vascular function using endothelial cell-specific *p53* deficient mice. We observed no changes in aerobic capacity, basal blood pressure, or endothelial mitochondrial phenotypes in the endothelial *p53* mull animals. However, after 7 weeks of voluntary wheel running exercise, blood pressure reduction and endothelial mitochondrial remodeling (biogenesis, elongation, and mtDNA replication) were substantially blunted in endothelial *p53* null animals compared to the wild-type, subjected to angiotensin II-induced hypertension. In addition, endothelial mtDNA lesions were significantly reduced following voluntary running exercise in wild-type mice, but not in the endothelial *p53* null mice. Moreover, *in vitro* studies demonstrated that unidirectional laminar flow exposure significantly increased key putative regulators for mitochondrial remodeling and reduced mitochondrial reactive oxygen species generation and mtDNA damage in a *p53*-dependent manner. Mechanistically, unidirectional laminar flow instigated translocalization of *p53* into the mitochondrial matrix where it binds to mitochondrial transcription factor A, *TFAM*, resulting in improving mtDNA integrity. Taken together, our findings suggest that *p53* plays an integral role in mitochondrial remodeling under physiological flow condition and the flow-induced *p53*-TFAM axis may be a novel molecular intersection for enhancing mitochondrial homeostasis in endothelial cells.

1. Introduction

Tumor suppressor *p53* resides in different compartments of the cell, including the mitochondria, cytosol, and nucleus, serving site-specific roles in maintaining mitochondrial integrity [1–3]. *P53* controls mitochondrial respiratory function by transcriptional and post-translational regulations of key regulatory proteins that are essential for mitochondrial biogenesis, mitochondrial fusion/fission, and mtDNA maintenance [4–9]. Mammalian mitochondrial transcription factor A (*TFAM*) is a nuclear-encoded high mobility group-box protein that plays an essential role in mtDNA quality control through the regulation of mtDNA replication and packaging [10–13]. *TFAM* directly binds to mtDNA at the

Abbreviations: UF, unidirectional flow; VW, voluntary running; SED, sedentary; EC, endothelial cell; iEC*p35*KO, inducible endothelial cell-specific *p53* knockout; WT, wild-type; AngII, angiotensin II; BP, blood pressure; TFAM, transcription factor A, mitochondrial; mtDNA, mitochondrial DNA; PhAM, photo-activatable mitochondria; Drp1, dynamin-related protein 1; POLγ, polymerase gamma; CHCHD4, coiled-coil-helix-coiled-coil-helix domain-containing protein 4.

* Corresponding author. Department of Kinesiology and Cardiovascular Research Center, Temple University, 1052 MERB, 3500 N. Broad Street, Philadelphia, PA, 19140, USA.
E-mail address: parkjy@temple.edu (J.-Y. Park).

[1] J.C.S. and S.G.H. contributed equally to this study.

https://doi.org/10.1016/j.redox.2022.102252
Received 11 January 2022; Received in revised form 25 January 2022; Accepted 26 January 2022
Available online 29 January 2022

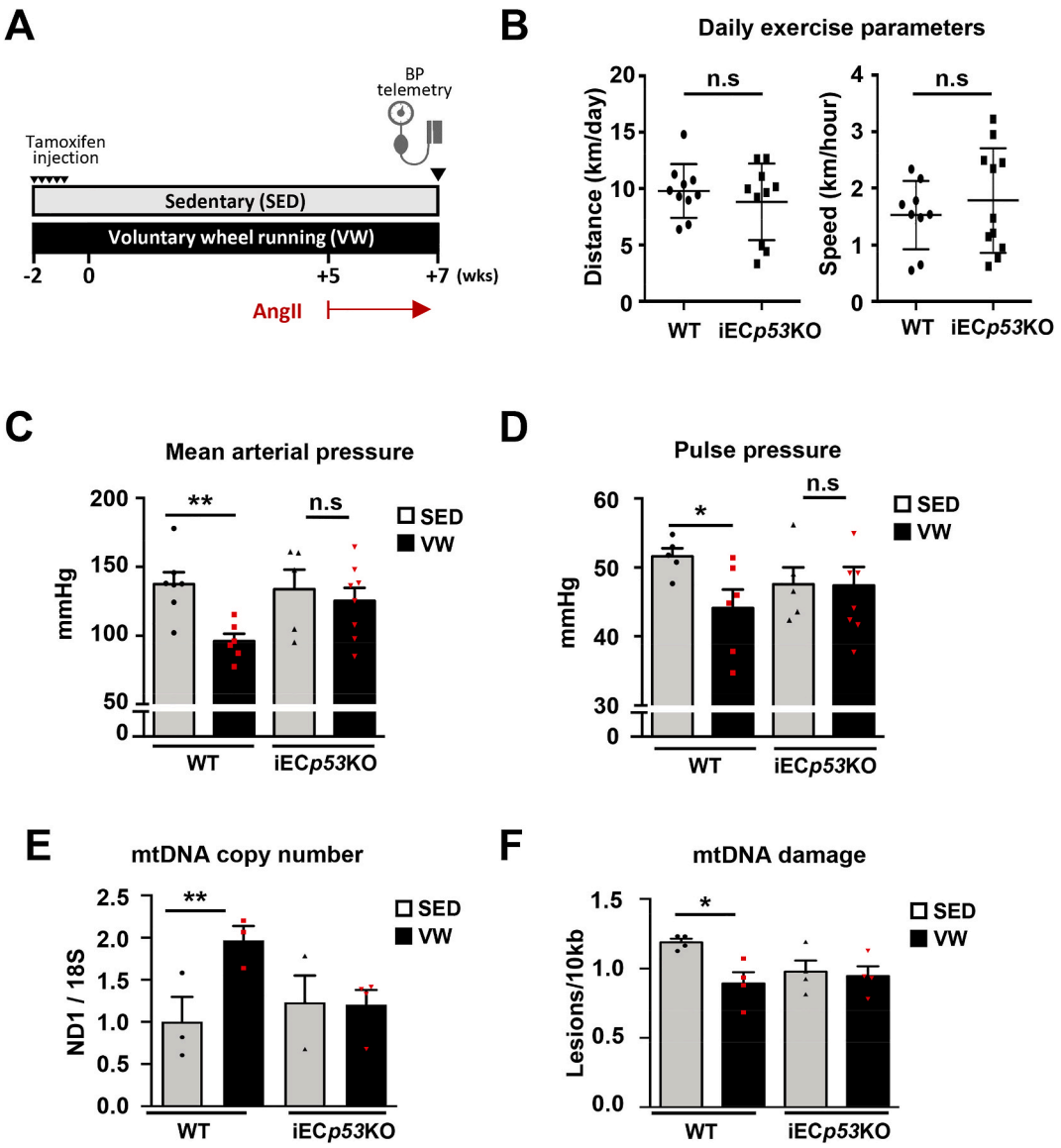

Fig. 1. Voluntary running reduces blood pressure in an endothelial p53-dependent manner in angiotensin II-induced hypertensive mice. (A) Experimental design. **(B)** Average daily running speed and distance of voluntary wheel running. **(C, D)** Bar graphs represent mean arterial pressure (MAP) and pulse pressure (PP). (n = 6–8). **(E)** mtDNA copy number assessed by the ratio between NDI (mitochondrial) and 18s rRNA (nuclear) content (n = 3–4). **(F)** mtDNA damage (n = 4). Data shown as means ± SEM. n.s., nonsignificant, *P < 0.05, **P < 0.01.

D-Loop in a sequence-specific fashion. *TFAM* also coats the entire mtDNA at an estimated rate of one molecule per 15–20 base pairs of the mitochondrial genome in a sequence-nonspecific fashion [14,15]. A previous study showed that removal of *p53* causes mtDNA depletion and mtDNA mutation through *TFAM*-dependent mechanisms, highlighting the importance of a *p53*-TFAM axis in maintaining mtDNA integrity [16].

Recent studies suggest that changes in the magnitude and pattern of fluid shear stress alter the mitochondrial content, shape, and intracellular distribution in ECs [17–19]. To this end, endurance aerobic exercise has been proven to be an effective physiological stimulus that remarkably modulates hemodynamic flow rate and patterns within the circulation [20,21].

Endothelial mitochondria are essential for protecting the functional integrity of ECs as they integrate a wide range of cellular processes [22,23]. Recently, it has been shown that diminished mitochondrial integrity exacerbates vascular disease progression. For instance, mitochondrial DNA (mtDNA) damage in the vessel has been shown to promote atherosclerosis [24], while mtDNA mutation has been associated with arterial stiffening and hypertension in *Polγ* mutant mice [25]. Additionally, elevated levels of damaged mtDNA in urine have been associated with hypertension; while restoring intact mtDNA copy number delays vascular aging phenotypes in the mitochondrial helicase *Twinkle* transgenic mice [26].

Hypertension affects one in every three adults in the US and is associated with an estimated 56 billion dollars in annual medical costs [27]. Worldwide, it has been estimated that approximately 7.8 million deaths and 143 million disability-adjusted life-years could be attributed to hypertension [28]. Despite currently available, multifaceted pharmacotherapeutic options, the global burden of both controlled and uncontrolled hypertension has ceaselessly risen over the past several decades [29,30]. Notably, physical inactivity has been recognized as the most prevalent modifiable risk factor for the development of hypertension [31,32]. Current guidelines invariably recommend increasing physical activity as one of the most potent lifestyle interventions to prevent hypertension [33–35]. To this end, it has been extensively studied that regular participation in physical activity effectively induces physiologic and metabolic adaptations in vascular, neural, and muscular

systems, which positively contribute to improving the regulation of blood pressure [36,37]. However, the molecular processes that elicit the protective effect of exercise on the vascular endothelial cells (ECs) are not fully understood. Therefore, the purpose of this study was to investigate the role of *p53* on flow-mediated mitochondrial remodeling in ECs and to determine the implication of the physical activity-induced adaptive cellular response in the prevention of hypertension.

2. Materials and methods

2.1. Animals experiments

All experiments were performed in accordance with the recommendations and the Guide for the Care and Use of Laboratory Animals of the National Institutes of Health and protocols approved by the Temple University Institutional Animal Care and Use Committee. To generate inducible EC specific-p53 knockout (iEC*p53*KO) mice, $p53^{flox/flox}$ mice (obtained from NCI Fredrick Mouse Repository) were intercrossed with Cre-inducible VE-Cadherin mice. Tamoxifen (Sigma Aldrich, #T5648) was administrated for 5 consecutive days via intraperitoneal injection (75 mg/kg/day) prior to experiments in order to generate a conditional knockout animal model (Fig. 1A). For all experiments, 8-16 week-old male mice were used. The EC-specific Dendra-2 photo-activatable mitochondria (EC-PhAM) mouse was generated by crossing VE-cadherin mice expressing Cre recombinase mice with PhAM floxed mice (The Jackson Laboratory) [38].

2.2. Voluntary running exercise

The 6–8 week old male mice were randomly assigned to either sedentary (SED) or voluntary wheel running exercise training (VW) groups (Fig. 1A). The mice in the VW group were individually housed in a cage equipped with a freely rotating running wheel with a diameter of 11.5 cm, while those assigned to the sedentary group were also housed individually in the same-sized cage without a running wheel. The average speed and duration of the voluntary exercise were regularly monitored by a magnetic counter installed on a running wheel.

2.3. Angiotensin II infusion

For angiotensin II (AngII) infusion, mice were anesthetized with isoflurane and AngII (1 mg/kg/day) was infused using a micro-osmotic pump (Alzet, #1002) for 2 weeks (The timeline is illustrated in Fig. 1A). Mice assigned to the control group underwent sham surgery on the same day as osmotic pump implantation.

2.4. Ambulatory blood pressure measures using implantable radio telemetry devices

Systolic blood pressure, mean arterial pressure, and pulse pressure were monitored using a radio telemetry device (PA-C10, Data Sciences International) at the end of the 7 weeks intervention period. The telemetry probe was implanted into the left carotid artery with anesthesia by a ketamine (90 mg/kg) and xylazine (5 mg/kg) combination. The mice were given 2 days in cages for recovery, and blood pressure was recorded by placing the cage on radio signal receiving plates.

2.5. Blood vessel preparation

Mice were euthanized 2 days after the end of 7-weeks of the VW exercise period. For the preparation of protein and DNA, the abdominal aorta was isolated after whole body perfusion with ice-cold PBS at a pressure of approximately 100 mmHg. For *en face* staining, the thoracic aorta was isolated after perfusion with ice-cold PBS and a fixative, 2% paraformaldehyde.

2.6. En face immunostaining and MitoSOX staining

Isolated blood vessels were post-fixed with 0.4% paraformaldehyde overnight at 4 °C. The vessels were then washed three times with PBS and incubated with 0.1 M glycine in 2% BSA/PBS for 30 min at room temperature. The fixed vessel samples were permeabilized using 0.3% Triton-X in 2% BSA/PBS for 30 min at room temperature. Mitochondrial contents were assessed using anti-HSP60 (Cell signaling, #D6F1) antibody and ECs were identified using anti-VE-Cadherin (Invitrogen, #14-1441-81) antibody. Primary antibodies were incubated overnight at 4 °C with gentle agitation. After rinsing three times with 2% BSA/PBS, secondary antibodies were incubated for 2 h at room temperature. Immunostained aorta samples were placed on slide glasses and cut longitudinally and mounted in DAPI fluoromount-G (Southern Biotech). Mitochondrial ROS production was measured using the fluorescent probe Mitosox Red mitochondrial superoxide indicator for live-cell imaging (Invitrogen, #M36008). Cells were incubated with Mitosox working solution (5 μM) for 15 min at 37 °C. The cells were gently washed three times with pre-warmed PBS after removal of the working solution. The images were collected using a fluorescence microscope (Axiomager, Zeiss or SP8 confocal microscope, Leica) with a 63X oil objective lens.

2.7. Immunostaining

For immunofluorescence staining, cells were fixed with 4% PFA for 15 min at room temperature and then washed with PBS three times. The fixed cells were then blocked with 10% normal goat serum in a staining buffer for 60 min at room temperature and subsequently incubated with primary antibodies in blocking buffer overnight at 4 °C. The cells were washed with PBS three times and incubated with secondary antibodies in staining buffer for 60 min at room temperature. The fluorescence images were obtained using a Zeiss inverted fluorescence microscope (Axio Observer Z1, Zeiss) with a 63X oil objective lens. Antibodies were from the following sources: TFAM (Novus, H00007019-B01P) and p53 (Santa Cruz, sc-126).

2.8. Mitochondrial fission count

Mitochondrial morphology was examined by mitochondrial fission count (MFC) as previously described [39]. Briefly, acquired images of mitochondria were imported into Image J and subjected to background subtraction and binary conversion to identify mitochondria segments. MFC was calculated by the number of individual mitochondria per cell divided by the total mitochondria area of a given cell (MFC = mitochondrial number/total mitochondrial area). An elevation of the MFC value represents more mitochondria per given area, indicating increased fission.

2.9. Cell culture and shear stress experiments

Human aortic endothelial cells (HAECs) were cultured in M199 media supplemented with 20% fetal bovine serum and EC growth supplement (Sigma-Aldrich, #E2759), and maintained at 37 °C under a humidified atmosphere containing 5% CO_2. Shear experiments were performed as previously described [20]. Briefly, prior to shear stress application, media was replaced with complete media containing 2% FBS. Laminar shear stress (20 dyne/cm^2) was applied to cells at 90–100% confluency for various durations indicated in the figure legend using a cone and plate viscometer (0.5° cone angle) or ibidi microfluidic pump system (ibidi GmbH).

2.10. Lentiviral vector production and transduction

HEK293T cells were transfected with either empty or p53 dominant-negative vector (Clontech, #631922) for 24 h with the FuGENE

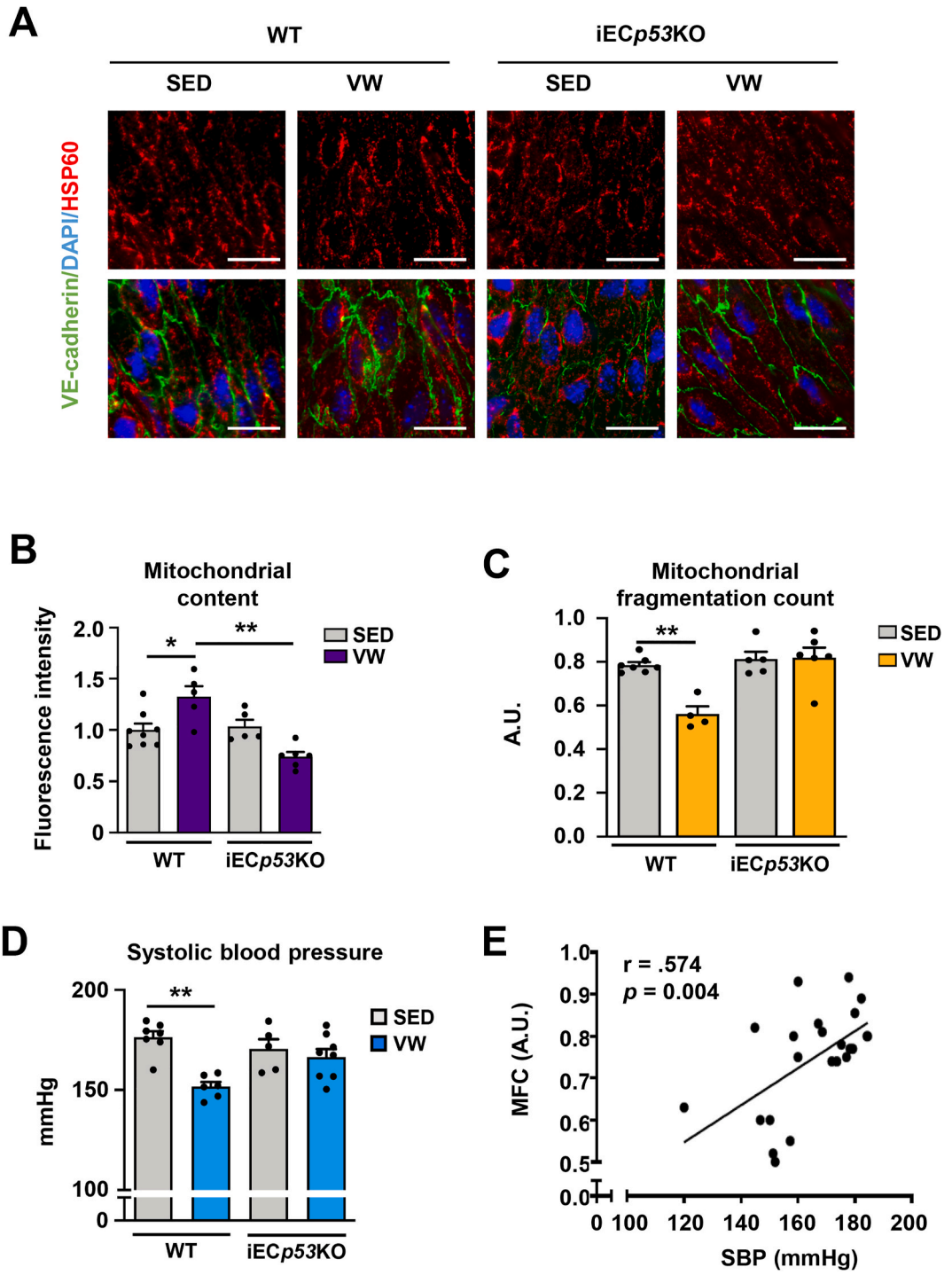

Fig. 2. Voluntary running induces mitochondrial remodeling in the endothelium in an endothelial p53-dependent fashion. **(A–C)** Morphological analyses of endothelial mitochondria. Representative microscopic images of *en face* staining of the thoracic aorta. n = 4–7 Immunostaining was performed for HSP60 (Red), VE-cadherin (Green), and DAPI (Blue). (n = 4–5) Scale bar = 25 μm. 1:630 magnification **(A)**. Quantification plot of mitochondrial content determined by HSP60 fluorescence intensity **(B).** Mitochondrial fission count **(C). (D)** Systolic blood pressure (SBP). **(E)** Correlation between SBP and mitochondria fragmentation (n=23). Data shown as means ± SEM. *P < 0.05, **P < 0.01. (For interpretation of the references to colour in this figure legend, the reader is referred to the Web version of this article.)

transfection agent (Promega) and Mission lentiviral packaging mix (Sigma, SHP001). HAECs were incubated with lentivirus particles (multiplicity of infection ~1) with hexadimethrine bromide (Sigma-Aldrich, #107689) for 24 h, followed by selection with 2 μl/ml puromycin (Sigma-Aldrich, #P8833).

2.11. mtDNA copy number assay

mtDNA copy number was determined by real-time qPCR as previously described [5]. Total genomic DNAs were isolated using the DNeasy kit (QIAGEN) and mtDNA contents were assessed by real-time qPCR. The relative ratio between mitochondrial DNA amount (COX I; cytochrome *c* oxidase subunit I or ND I; NADH dehydrogenase subunit 1)

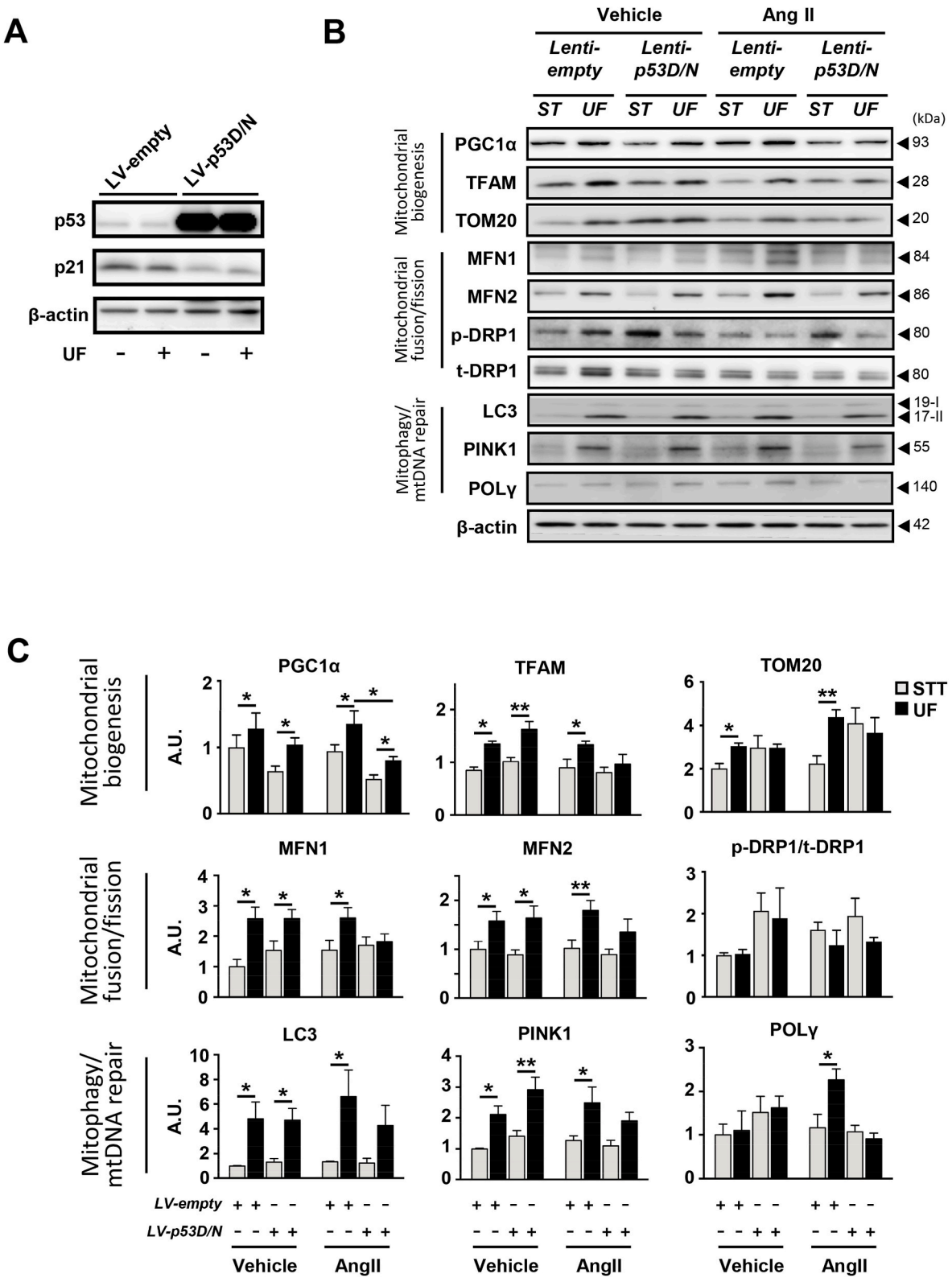

Fig. 3. Unidirectional laminar flow upregulates key mitochondrial regulatory proteins in a p53-dependent manner. (A) Representative immunoblot images of p53 and p21 expression in HAECs transduced with lentiviral p53 dominant-negative or empty vector control. **(B)** Representative immunoblot images for the protein expression related to mtDNA biogenesis (PGC-1α, TFAM, TOM20), mitochondrial fusion/fission (MFN1, MFN2, *p*-DRP1 Ser637, t-DRP1), mitophagy (LC3, PINK1) and mtDNA repair (POLγ) in HAECs under static or unidirectional flow (20 dyn/cm^2, 48 h). AngII treatment (200 nM for 6 h). β-actin was used as the loading control. **(C)** Quantification plots (n = 3–5 per group). Data shown as means ± SEM. *P < 0.05, **P < 0.01.

compared to nuclear DNA (18s rRNA) amount was calculated. Primer sequences are as follows: ND1, F:5′- CCCTAAAACCCGCCACATCT-3′, R:5′- GAGCGATGGTGAGAGCTAAGGT-3'; COXI, F:5′-CAGGTTTATGGA GGGTTCTTC-3′, R:5′-CATAGGAGGCTTCATTCACTG-3'. 18s rRNA, F: 5′-CTTAGAGGGACAAGTGGCGTTC-3′, F:5′-GCTGAGCCAGTCAGTGTA G-3'.

2.11.1. mtDNA lesion assay

Fifteen nanograms of purified DNA from each sample were amplified with LongAmp Hot Start Tag 2X Master Mix polymerase Taq (NEB, #M0533S) for long amplicon (LA) and short amplicon (SA). The PCR products were quantified using PicoGreen dye using a fluorescence plate reader (excitation and emission wavelengths were 485 and 528 nm, respectively; TECAN, Infinite M1000Pro). The LA and SA respective fluorescence values were analyzed to determine the lesion frequency per fragment at dose $D=-\ln A_D/A_O$, where A_D represents the number of damaged DNA amplicons (Long PCR) and A_O is undamaged DNA amplicons (Short PCR) [40,41]. mtDNA damage was expressed as lesions per kilobase. Primer sequences are as follows. *Human* 8.9 kb mtDNA fragment: F:5′-TCTAAGCCTCCTTATTCGAGCCGA-3′, R:5′-TT TCATCATGCGGAGATGTTGGATGG-3'; 248 bp mtDNA fragment: F:5′-CCCCACAAACCCCATTACTAAACCCA-3′, R: 5′-TTTCATCATGCG-GAGATGTTGGATGG-3'. *Mouse* 10 kb mtDNA fragment F:5′-GCCAGC CTGACCCATAGCCATAATAT-3′, R:5′-GAGAGATTTTATGGGTGTAATG CGG-3'; 117-bp mtDNA fragment: F:5′-CCCAGCTACTACCATCA TTCAAGT-3′, R:5′- GATGGTTTGGGAGATTGGTTGATGT-3'.

2.12. Duolink proximity ligation assay

The Duolink proximity ligation assay was carried out according to the manufacturer's protocol (Sigma Aldrich, #DUO92101). Briefly, HAECs were grown on 8-well chamber slides or ibidi μ-slides. Cells were fixed with 4% paraformaldehyde for 15 min at room temperature. After washing with PBS, the cells were blocked in Duolink blocking solution for 60 min at 37 °C and then incubated with primary antibody (α-P53 and α-Tfam) diluted in Duolink Antibody Diluent overnight at 4 °C. Samples were mounted using Duolink in Situ Mounting Media with DAPI. The fluorescence images were obtained using a Zeiss inverted fluorescence microscope (Axio Observer Z1, Zeiss) with a 63X oil objective lens. It is well known that transcription factors often demonstrate low temporal expression that nevertheless plays a critical functional roles. Therefore, for the quantitative analysis, we analyzed more than 150 cells per each STT and UF conditions.

2.13. Western blot

Protein samples were homogenized in ice-cold RIPA lysis buffer with phosphatase inhibitor (Sigma-Aldrich, #04906845001) and protease inhibitor (ThermoFisher, #87785). Lysed cells were incubated on ice for 20 min and centrifuged at 13,500g for 20 min at 4 °C. Collected supernatants were subjected to a Pierce BCA protein assay (ThermoFisher, #23225) to quantify protein concentration. The lysate samples were separated via Novex 4–20% Tris-Glycine gel and transferred to an immobilon-P membrane (Millipore). The membrane was visualized by standard enhanced chemiluminescence. Antibodies were from the following sources: VDAC1 (abcam, ab15895), Histone H3 (abcam, ab1791), MFN1 (abcam, ab57602), MFN2 (Santa Cruz, sc-100560), β-actin (Sigma-Aldrich, A1978), DRP1 (BD Biosciences, 610296), pDRP1 Ser637 (Cell signaling technology, #6319), Tom20 (Cell signaling technology, #42406), TFAM (Novus, H00007019-B01P), p53 (Santa Cruz, sc-126), PINK1 (Cell signaling technology, #6964), LC3B (Santa Cruz, sc-16755), p21 (Cell signaling technology, #2947) and Polymerase gamma (Novus, #NBP1-52300), CHCHD4 (ProteinTech, #21090-1-AP), PGC-1α (Novus, P1-04676).

2.14. Co-immunoprecipitation

Dynabeads Co-Immunoprecipitation system (Life Technologies, 14321D) was used to carry out co-immunoprecipitation by following the manufacturer's protocol. For antibody coupling, 5 μg of antibody per mg bead was used, and incubated at 37 °C for 16–24 h. The extracted protein was resuspended with 1.5 mg of antibody-coupled beads at 4 °C for 40 min on a rotator. The protein complex was resuspended with Elution Buffer, and the supernatant was collected on a magnet field.

2.15. Statistics

All results are presented as mean ± SEM. All probability values were calculated using 2-tailed distribution Student's t-test and considered to be significant if $p<0.05$. One-way analysis of variance (ANOVA) followed by Tukey's post hoc test or Fisher's LSD test were used for comparisons among the different genotype groups. The correlation coefficient was used to measure the strength of a linear association between two variables. All statistical analyses were performed using SPSS statistical software.

3. Results

3.1. Voluntary exercise-induced endothelial mitochondrial remodeling and reduced blood pressure in a p53-dependent manner in angiotensin II-induced hypertensive mice

We examined mitochondrial content and shape *in vivo* in the *en face* preparations of thoracic aortas which previously showed the biggest changes in mitochondrial biogenic response to exercise training [21]. For these experiments, mice were subjected to AngII or saline infusion while housed in either regular or voluntary wheel cages as illustrated in Fig. 1A. During the 7-week period of voluntary running, daily running distance (~10 km/day) and average running speed (~1.8 km/h) were similar between iEC*p53*KO and WT mice (Fig. 1B). In the endothelium, mitochondrial content, determined by mitochondrial 60 KDa heat shock protein (HSP60) abundance [42], was significantly increased in the WT, but not in the iEC*p53*KO under an AngII-induced hypertensive condition (Fig. 2A and B). Further analysis of the mitochondrial morphology indicated that mitochondrial fission count was significantly lower in the VW group in WT mice, indicating an enhanced mitochondrial network (fusion), but this change was disappeared in the iEC*p53*KO mice (Fig. 2C). The degree of endothelial mitochondrial fragmentation was significantly correlated with systolic blood pressure (Fig. 2D and E). Furthermore, we measured ambulatory blood pressure from these mice at the end of the study using implantable radio telemetry devices and observed significant reductions in both mean arterial pressure (~25.8%) and pulse pressure (~27.0%) in WT mice (Fig. 1C and D). However, there were no significant reductions in both parameters in iEC*p53*KO mice following the voluntary running exercise. Similarly, mtDNA copy number was significantly elevated following VW training in WT mice, but no significant changes were observed in iEC*p53*KO mice (Fig. 1E). VW training significantly suppressed mtDNA lesions in the angiotensin II-induced hypertensive aortic tissues in a p53-dependent fashion (Fig. 1F).

3.2. Unidirectional laminar flow increases putative regulators for mitochondrial remodeling, reduces mtROS generation, and mitigates mtDNA damage in a p53-dependent manner

Next, we investigated whether p53 regulates regulatory proteins related to mitochondria biogenesis, mitochondrial fusion/fission, mitophagy, mtDNA replication, and mtDNA repair under unidirectional laminar flow (UF) (Fig. 3). For these experiments, we employed a lentiviral system containing either a dominant-negative (D/N) p53 (pLEX-p53mt135) system, and an empty vector (pLEX) was used as a control.

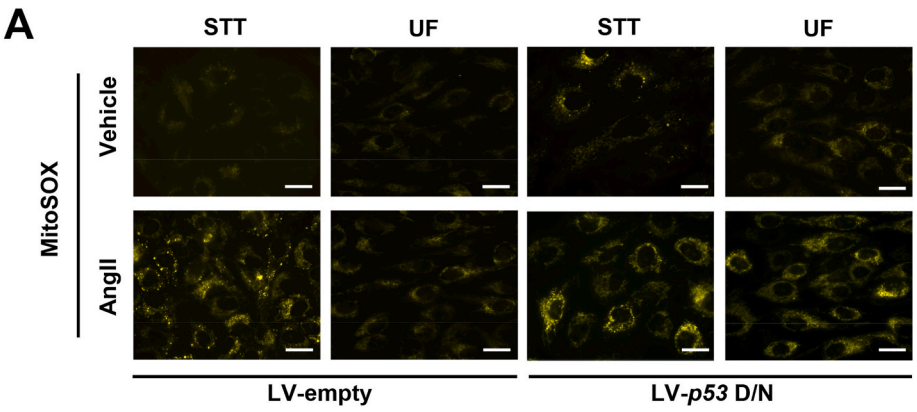

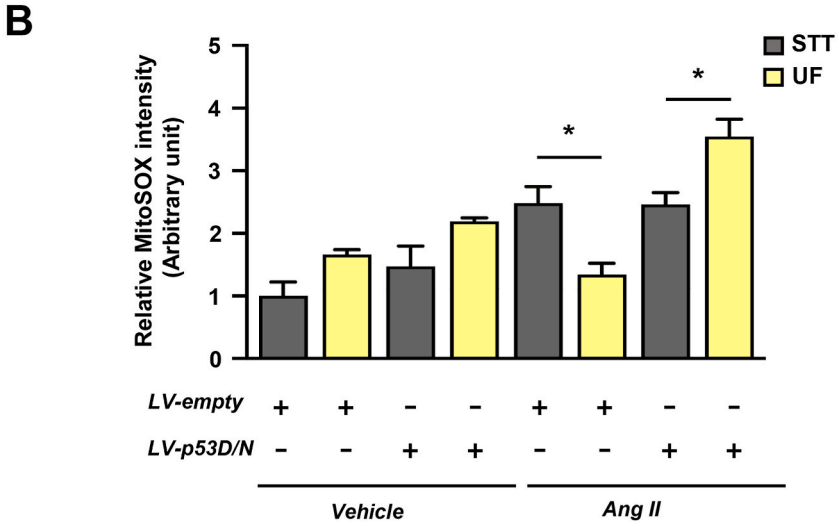

Fig. 4. Unidirectional laminar flow reduces angiotensin II-induced mtROS production in a p53-dependent manner. (A) Representative micrographs of MitoSOX staining. mtROS production determined by Mitosox™ staining under static or unidirectional flow (20 dyn/cm^2, 48 h) conditions with saline or AngII treatment (6 h) (n = 3). Scale bar = 25 μm. 1:630 magnification. **(B)** Quantification of fluorescence intensity (n = 3). Data shown as means ± SEM. *P < 0.05, **P < 0.01.

P21, a well-described p53 downstream target, the expression level was drastically suppressed in LV-p53D/N transduced HAECs, validating the efficiency of the lentiviral system (Fig. 3A). UF significantly increased the expression of mitochondrial proteins associated with mitochondrial biogenesis (PGC1α, TFAM, TOM20), mitochondrial fusion (MFN1 and MFN2), mitophagy (LC3 and PINK1), and mtDNA maintenance (POLγ) under, especially, AngII treatment condition in a p53-dependent fashion. Mitochondrial fission protein, dynamin-related protein 1 (Drp1), was not affected by UF (Fig. 3B and C). UF also significantly reduced mtROS production, determined by MitoSOX™ staining, in a p53-dependent fashion in AngII-treated HAECs (Fig. 4). Furthermore, while UF significantly reduced mtDNA lesion (Fig. 5A) and increased mtDNA content (Fig. 5B), these changes were abolished in p53D/N ECs.

3.3. *Unidirectional laminar flow induces mitochondrial translocation of p53 and promotes P53-TFAM interaction*

As shown in Fig. 6A and B, the level of cytosolic p53 was significantly increased after exposure to UF in HAECs. To further validate the intracellular distribution of p53, we measured the levels of p53 in nuclear, mitochondrial, and cytosolic fractions under static or UF conditions. Mitochondrially localized p53 levels were increased up to ~35% following UF exposure, while the nuclear and cytosolic levels were proportionally decreased under UF (Fig. 6C & D). Next, we examined the intracellular distribution of p53 *in vivo* through *en face* staining of the thoracic aortas with or without voluntary exercise, a shear stress mimetic, in EC-PhAM mice (Fig. 6E and F). The level of mitochondrial p53 was significantly higher in VW mice compared to sedentary controls while nuclear p53 level was proportionally lower in the VW mice. The shear-induced p53 and TFAM interaction was analyzed by proximity ligation assay and co-immunostaining. p53/TFAM co-localization signal was significantly increased under UF compared to the static control (Fig. 7A and B), which is confirmed by proximity ligation assay showing a greater ^{mito}p53-TFAM physical interaction (Fig. 7C and D).

4. Discussion

Studies in the past several decades have emphasized the importance of physical activity to prevent cardiovascular disease, however, the molecular mechanisms involved in the observed vascular protective effects are incompletely understood. In this study, we provided a novel insight into the role of p53 on mitochondrial adaptations to unidirectional laminar flow in ECs. In the present study, data suggest that 1) p53 promotes mitochondrial biogenesis, mitochondrial networking, and mtDNA integrity in the endothelium following voluntary running exercise training; 2) the blood pressure-lowering effect of the voluntary exercise is mediated by endothelial p53; 3) UF upregulates putative regulators of mitochondrial remodeling (biogenesis, dynamics, and mitophagy) and mtDNA repair in a p53-dependent fashion; 4) UF induces translocalization of p53 into the mitochondria and promotes the p53-TFAM interaction.

This study is the first to illustrate that iEC*p53*KO mice showed blunted training effects on blood pressure control. Our data suggest that the exercise training effects are achieved, at least in part, by translocated

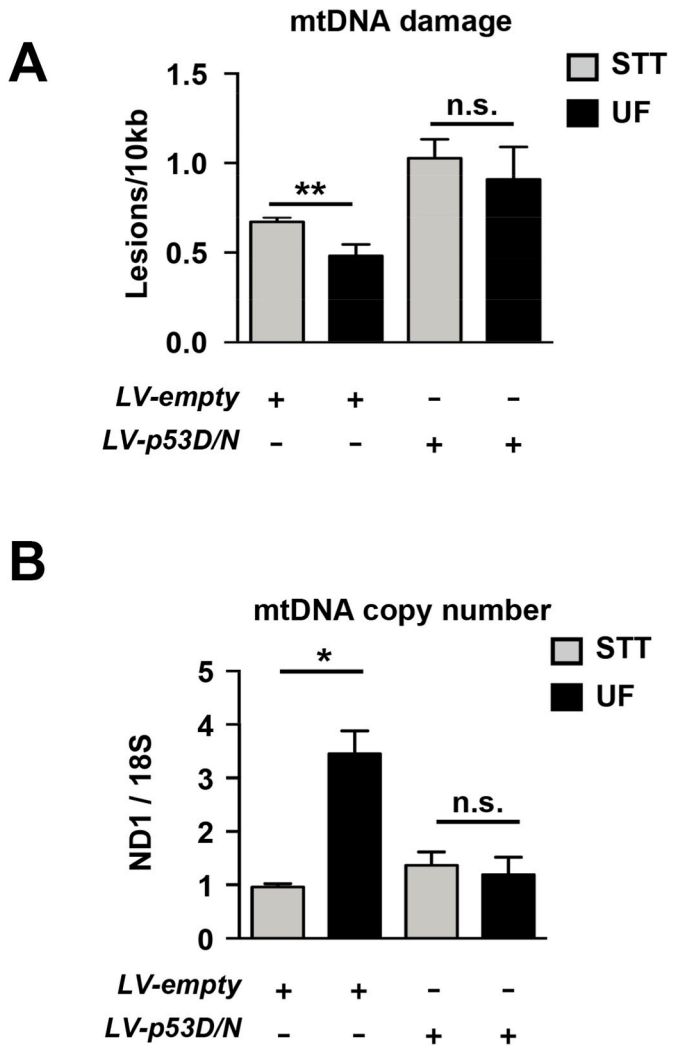

Fig. 5. Unidirectional laminar flow mitigates mtDNA damage in a p53-dependent fashion. **(A)** mtDNA lesion. mtDNA lesion counts were assessed after AngII treatment (6h) under static (STT) or unidirectional flow (20 dyn/cm^2, 48h) (n = 4–5). **(B)** mtDNA copy number assessed by the ratio between COXI (mitochondrial) and 18s rRNA (nuclear) content (n = 3–4). Data shown as means ± SEM. n.s., nonsignificant, *P < 0.05, **P < 0.01.

nuclear and cytosolic p53 into the mitochondrial matrix which promotes p53/TFAM/mtDNA interaction in the ECs. Moreover, we found that mitochondrial fragmentation in the thoracic aorta endothelium that was correlated with AngII-induced elevation of blood pressure was significantly reduced by VW training. Together, data suggest that p53 is likely to contribute to the exercise training-mediated blood pressure lowering effect by enhancing p53-TFAM interaction within the mitochondria. While we posit that these are novel and exciting findings, the precise molecular mechanism by which iEC*p53*KO mice demonstrate reduced adaptive responses to exercise training warrants further research.

In this study, we report that endothelial p53 is translocalized into mitochondria, specifically to the mitochondrial matrix, under UF; then, it facilitates interaction with TFAM. Tumor suppressor p53 is known as an important transcription factor involved in mitochondrial respiration, mtDNA repair, and mitophagy [4,43,44]. TFAM is an essential regulator for mitochondrial replication and transcription in the context of mtDNA maintenance mechanism [8,45]. A previous study showed that the physical interaction between p53 and TFAM is important for stabilizing TFAM, and it is required process to confer replication of mtDNA [8]. Studies have also shown that TFAM directly binds with the mtDNA duplex and protects mtDNA from oxidative damages thereby maintaining mtDNA quality [15]. We observed that TFAM protein expression level was not influenced by p53 dominant-negative (D/N) transduction, suggesting that UF enhanced TFAM activity in a p53-dependent manner. Further insight into the molecular processes underlying the improved TFAM activity warrants future study.

Previous studies demonstrated that subcellular distribution of p53 in nuclear, cytosol, and mitochondrial compartments can be altered by altering physiological conditions [1,2,7]. Herein, we examined whether a physiological level of UF regulate intracellular partitioning of p53 in ECs, resulting in the accumulation of p53 in the mitochondria. Well-characterized binding partners of mitochondrial p53 include B-cell lymphoma 2 (Bcl-2) family members Bcl-2, B-cell lymphoma-extra-large (Bcl-xL) and Bcl-2 homologous antagonist/killer (Bak), and their interaction has been shown to result in programmed cell death by the formation of mitochondrial outer membrane permeabilization. However, this notion contradicts the apoptosis-suppressing effect of UF, which has been previously documented. Thus, we explored other potential binding partners including POLγ, CHCHD4 (a mammalian homologous of mia40), and TFAM, and we observed that binding activity of p53 with TFAM, but not with POLγ or CHCHD4, is increased by UF exposure (no data shown).

In this study, we found that voluntary training *in vivo* or unidirectional laminar flow *in vitro* seemed to promote mtDNA replication in ECs in a p53-TFAM-dependent fashion [20,21]. We also report, here, that flow-preconditioning significantly alleviated AngII induced-mtDNA damage and reduced mtROS generation in ECs in a p53-dependent manner. These data suggest that the inactivation of p53 detracted the effect of exercise (or UF) especially on its effects on endothelial mitochondrial biogenesis and mtDNA replication. Interestingly, UF upregulated POLγ, which is one of the crucial polymerases for mtDNA repair and replication [46,47]. The specific mechanisms by which POLγ contributes to flow-mediated mtDNA repair system in ECs needs to be further elucidated.

5. Conclusion

The present study provides novel evidence that p53 is a crucial mediator of the endothelium's adaptive response to exercise training or laminar shear stress in connection with mitochondria function under pathological conditions. Furthermore, we report here, that exercise-mediated unidirectional laminar flow enhances mitochondrial integrity by promoting mitochondrial remodeling and mtDNA quality control, and that endothelial p53 plays a pivotal role in the adaptive response to exercise. These data may shed new light on a novel cellular mechanism for the development of hypertension, which would potentially provide the basic mechanistic insights, helping to develop a prevention strategy to curve this public health epidemic.

Data availability statement

The raw data supporting the conclusions of this article will be made available by the corresponding author/s.

Ethics statement

The animal study was reviewed and approved by the Temple University Institutional Animal Care and Use Committee.

Author contributions

JCS, SGH, and JYP conceived the study. SYC, SGJ, and JS obtained the data. SE, VR, RS, and JYP participated in data interpretation and discussed the results. JCS, SGH, and SYC primarily drafted the manuscript and constructed figures. DGJ, JS, and HSP provided critical

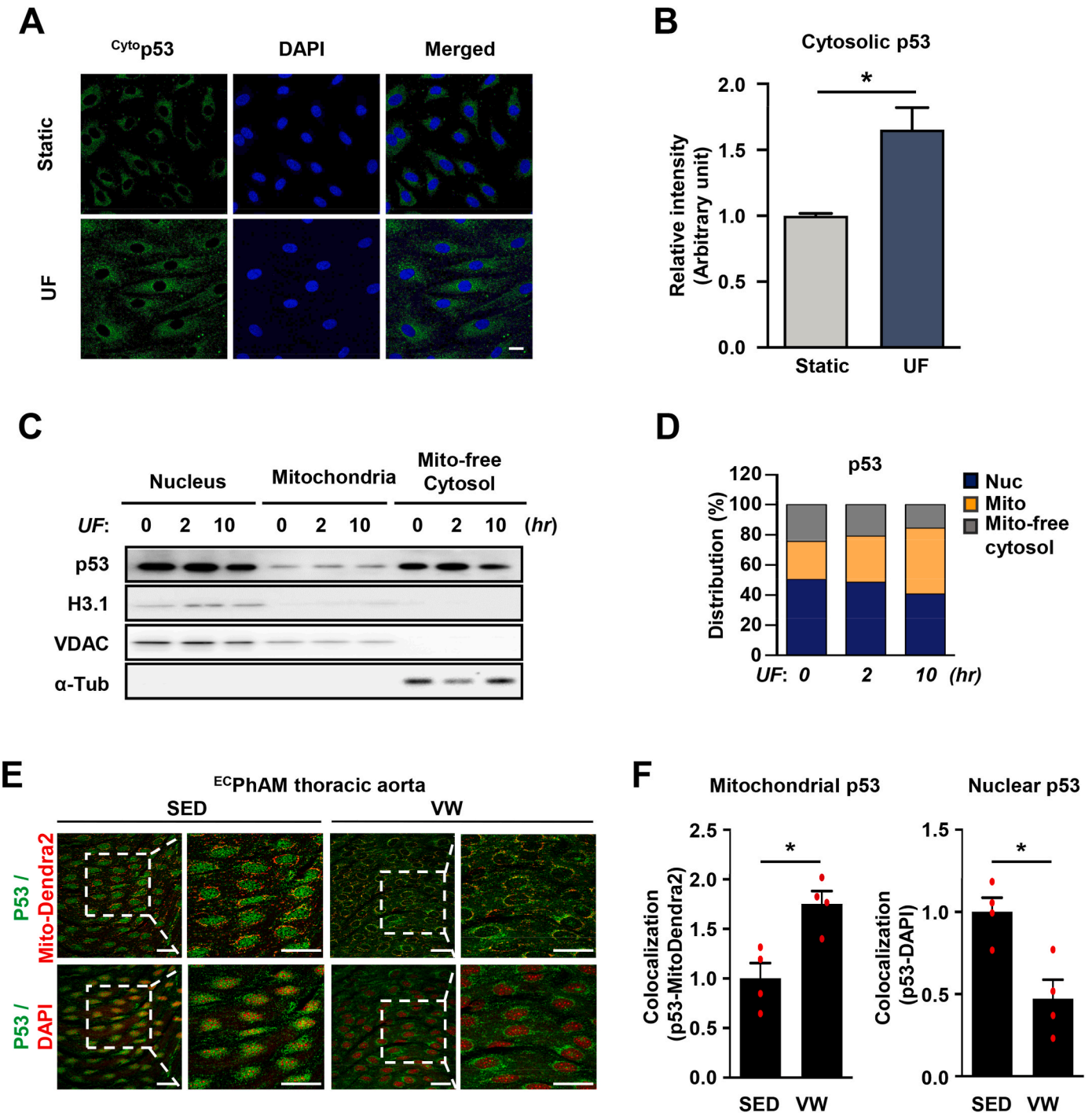

Fig. 6. Unidirectional laminar flow induces mitochondrial translocation of p53. **(A)** Representative microscopic images. **(B)** Quantification plot of cytosolic p53 in HAECs under static (STT) or unidirectional flow (UF, 20 dyn/cm^2, 6h) (n = 3). **(C)** Representative immunoblot images for p53 in fractionated cell compartments. **(D)** Quantification plot of p53 in nuclear, mitochondrial, or cytosolic fractions with unidirectional flow (20 dyn/cm2, 2 or 10 h). **(E)** Representative confocal microscopic images of *en face* staining. P53 (green), mitochondria (red, upper) and nucleus (red, bottom) were determined in the thoracic aorta of EC-specific PhAM mice (^{EC}PhAM). Scale bar = 25 μm. 1:630 magnification. **(F)** Quantification plots of colocalization of p53-mitoDendra2 (left panel) and p53-DAPI (right panel) (n = 4). Data shown as means ± SEM. *P < 0.05, **P < 0.01. (For interpretation of the references to colour in this figure legend, the reader is referred to the Web version of this article.)

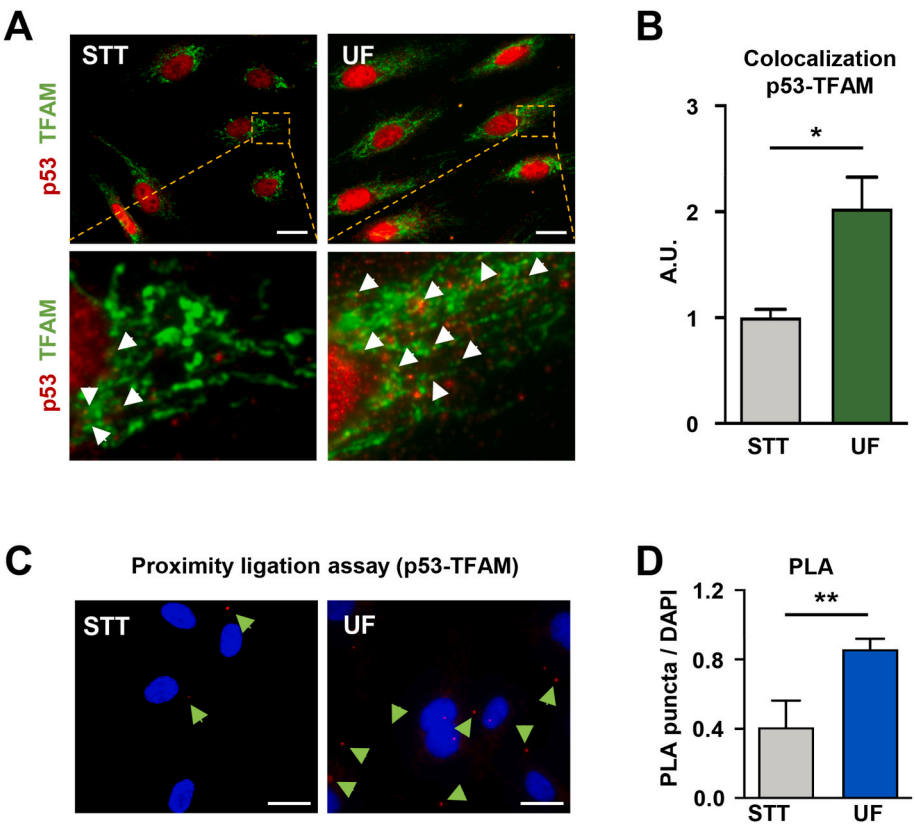

Fig. 7. Unidirectional laminar flow promotes p53-TFAM interaction in HAECs. (A, B) Representative images (right panel) and quantification plot (left panel) of co-localization between p53 and TFAM under STT or UF (20 dyn/cm^2, 6h) condition in HAECs. Scale bar = 25 μm. 1:630 magnification. Data shown as means ± SEM. *P < 0.05, **P < 0.01. **(C, D)** Representative images for proximity ligation assay (PLA) (A) and quantification plot (B). The p53-TFAM physical interactions were assessed under unidirectional flow (UF, 20 dyn/cm^2, 6 h) or static (STT) flow in HAECs. (Scale bar = 25 μM). 1:630 magnification.

assistance in manuscript preparation. HW, SRH, and JYP edited the manuscript. All authors edited the manuscript, and all authors approved the final submitted version.

Funding

This work was supported by funding from the National Institutes of Health, United States (R01HL126952) and the American Heart Association, United States (12SDG12070327). Dr. Shin was supported by an award from the American Heart Association and the Beatrice F. Nicoletti Post-Doctoral Research Fellowship, United States (19POST34450157).

Declaration of competing interest

The authors declare that the research was conducted in the absence of any commercial or financial relationships that could be construed as a potential conflict of interest.

Acknowledgements

We are grateful to the technical assistance of Katherine J. Elliott, Jamie Seo and Huimin Shan.

References

[1] J. Zhuang, et al., Forkhead box O3A (FOXO3) and the mitochondrial disulfide relay carrier (CHCHD4) regulate p53 protein nuclear activity in response to exercise, J. Biol. Chem. 291 (2016) 24819–24827.
[2] A. Safdar, et al., Exercise-induced mitochondrial p53 repairs mtDNA mutations in mutator mice, Skeletal Muscle 6 (2016) 7.
[3] C.A. Koczor, et al., p53 and mitochondrial DNA: their role in mitochondrial homeostasis and toxicity of antiretrovirals, Am. J. Pathol. 180 (2012) 2276–2283.
[4] S. Matoba, et al., p53 regulates mitochondrial respiration, Science 312 (2006) 1650–1653.
[5] J.Y. Park, et al., p53 improves aerobic exercise capacity and augments skeletal muscle mitochondrial DNA content, Circ. Res. 105 (2009) 705–712, 711 pp. following 712.
[6] G. Achanta, et al., Novel role of p53 in maintaining mitochondrial genetic stability through interaction with DNA Pol gamma, EMBO J. 24 (2005) 3482–3492.
[7] A. Saleem, D.A. Hood, Acute exercise induces tumour suppressor protein p53 translocation to the mitochondria and promotes a p53-Tfam-mitochondrial DNA complex in skeletal muscle, J. Physiol. 591 (2013) 3625–3636.
[8] Y. Yoshida, et al., P53 physically interacts with mitochondrial transcription factor A and differentially regulates binding to damaged DNA, Cancer Res. 63 (2003) 3729–3734.
[9] W. Wang, et al., Mitofusin-2 is a novel direct target of p53, Biochem. Biophys. Res. Commun. 400 (2010) 587–592.
[10] N.G. Larsson, et al., Mitochondrial transcription factor A is necessary for mtDNA maintenance and embryogenesis in mice, Nat. Genet. 18 (1998) 231–236.
[11] R.C. Scarpulla, Transcriptional paradigms in mammalian mitochondrial biogenesis and function, Physiol. Rev. 88 (2008) 611–638.
[12] M.I. Ekstrand, et al., Mitochondrial transcription factor A regulates mtDNA copy number in mammals, Hum. Mol. Genet. 13 (2004) 935–944.
[13] B.A. Kaufman, et al., The mitochondrial transcription factor TFAM coordinates the assembly of multiple DNA molecules into nucleoid-like structures, Mol. Biol. Cell 18 (2007) 3225–3236.
[14] B.M. Hallberg, N.G. Larsson, TFAM forces mtDNA to make a U-turn, Nat. Struct. Mol. Biol. 18 (2011) 1179–1181.
[15] C. Kukat, et al., Cross-strand binding of TFAM to a single mtDNA molecule forms the mitochondrial nucleoid, Proc. Natl. Acad. Sci. U. S. A. 112 (2015) 11288–11293.
[16] M.A. Lebedeva, J.S. Eaton, G.S. Shadel, Loss of p53 causes mitochondrial DNA depletion and altered mitochondrial reactive oxygen species homeostasis, Biochim. Biophys. Acta 1787 (2009) 328–334.
[17] K. Yamamoto, H. Imamura, J. Ando, Shear stress augments mitochondrial ATP generation that triggers ATP release and Ca(2+) signaling in vascular endothelial cells, Am. J. Physiol. Heart Circ. Physiol. 315 (2018) H1477–H1485.
[18] Z. Chen, et al., Shear stress, SIRT1, and vascular homeostasis, Proc. Natl. Acad. Sci. U. S. A. 107 (2010) 10268–10273.
[19] L.H. Wu, H.C. Chang, P.C. Ting, D.L. Wang, Laminar shear stress promotes mitochondrial homeostasis in endothelial cells, J. Cell. Physiol. 233 (2018) 5058–5069.
[20] J.S. Kim, et al., Shear stress-induced mitochondrial biogenesis decreases the release of microparticles from endothelial cells, Am. J. Physiol. Heart Circ. Physiol. 309 (2015) H425–H433.
[21] B. Kim, H. Lee, K. Kawata, J.Y. Park, Exercise-mediated wall shear stress increases mitochondrial biogenesis in vascular endothelium, PLoS One 9 (2014), e111409.
[22] S. Caja, J.A. Enriquez, Mitochondria in endothelial cells: sensors and integrators of environmental cues, Redox Biol. 12 (2017) 821–827.
[23] M.A. Kluge, J.L. Fetterman, J.A. Vita, Mitochondria and endothelial function, Circ. Res. 112 (2013) 1171–1188.

[24] E.P. Yu, M.R. Bennett, The role of mitochondrial DNA damage in the development of atherosclerosis, Free Radic. Biol. Med. 100 (2016) 223–230.
[25] M.J. Golob, et al., Mitochondria DNA mutations cause sex-dependent development of hypertension and alterations in cardiovascular function, J. Biomech. 48 (2015) 405–412.
[26] K. Foote, et al., Restoring mitochondrial DNA copy number preserves mitochondrial function and delays vascular aging in mice, Aging Cell 17 (2018), e12773.
[27] E.J. Benjamin, et al., Heart disease and stroke statistics-2019 update: a report from the American Heart association, Circulation 139 (2019) e56–e528.
[28] M.H. Forouzanfar, et al., Global burden of hypertension and systolic blood pressure of at least 110 to 115 mm Hg, 1990-2015, JAMA 317 (2017) 165–182.
[29] K.S. Dorans, K.T. Mills, Y. Liu, J. He, Trends in prevalence and control of hypertension according to the 2017 American college of cardiology/American Heart association (ACC/AHA) guideline, J. Am. Heart Assoc. 7 (2018).
[30] R.M. Carey, S. Sakhuja, D.A. Calhoun, P.K. Whelton, P. Muntner, Prevalence of apparent treatment-resistant hypertension in the United States, Hypertension 73 (2019) 424–431.
[31] M.R. Carnethon, et al., Joint associations of physical activity and aerobic fitness on the development of incident hypertension: coronary artery risk development in young adults, Hypertension 56 (2010) 49–55.
[32] N.L. Chase, X. Sui, D.C. Lee, S.N. Blair, The association of cardiorespiratory fitness and physical activity with incidence of hypertension in men, Am. J. Hypertens. 22 (2009) 417–424.
[33] P.K. Whelton, et al., Guideline for the prevention, detection, evaluation, and management of high blood pressure in adults: executive summary: a report of the American college of cardiology/American Heart association task force on clinical practice guidelines, Hypertension 71 (2017) 1269–1324. ACC/AHA/AAPA/ABC/ACPM/AGS/APhA/ASH/ASPC/NMA/PCNA, 2018.
[34] B. Williams, et al., ESC/ESH Guidelines for the management of arterial hypertension, Eur. Heart J. 39 (2018) 3021–3104, 2018.
[35] L.S. Pescatello, et al., American College of Sports Medicine position stand. Exercise and hypertension, Med. Sci. Sports Exerc. 36 (2004) 533–553.
[36] C.A. DeSouza, et al., Regular aerobic exercise prevents and restores age-related declines in endothelium-dependent vasodilation in healthy men, Circulation 102 (2000) 1351–1357.
[37] E.P. Delaney, et al., Exaggerated sympathetic and pressor responses to handgrip exercise in older hypertensive humans: role of the muscle metaboreflex, Am. J. Physiol. Heart Circ. Physiol. 299 (2010) H1318–H1327.
[38] A.H. Pham, J.M. McCaffery, D.C. Chan, Mouse lines with photo-activatable mitochondria to study mitochondrial dynamics, Genesis 50 (2012) 833–843.
[39] Z. Hong, et al., Role of dynamin-related protein 1 (Drp1)-mediated mitochondrial fission in oxygen sensing and constriction of the ductus arteriosus, Circ. Res. 112 (2013) 802–815.
[40] A. Furda, J.H. Santos, J.N. Meyer, B. Van Houten, Quantitative PCR-based measurement of nuclear and mitochondrial DNA damage and repair in mammalian cells, Methods Mol. Biol. 1105 (2014) 419–437.
[41] C.P. Gonzalez-Hunt, et al., PCR-based analysis of mitochondrial DNA copy number, mitochondrial DNA damage, and nuclear DNA damage, Curr. Protoc. Toxicol. 67 (2016) 20 11 21–20 11 25.
[42] M. Laforge, et al., NF-kappaB pathway controls mitochondrial dynamics, Cell Death Differ. 23 (2016) 89–98.
[43] C.Q. Dai, et al., p53 and mitochondrial dysfunction: novel insight of neurodegenerative diseases, J. Bioenerg. Biomembr. 48 (2016) 337–347.
[44] J.H. Park, J. Zhuang, J. Li, P.M. Hwang, p53 as guardian of the mitochondrial genome, FEBS Lett. 590 (2016) 924–934.
[45] T.S. Wong, et al., Biophysical characterizations of human mitochondrial transcription factor A and its binding to tumor suppressor p53, Nucleic Acids Res. 37 (2009) 6765–6783.
[46] N. Nissanka, S.R. Bacman, M.J. Plastini, C.T. Moraes, The mitochondrial DNA polymerase gamma degrades linear DNA fragments precluding the formation of deletions, Nat. Commun. 9 (2018) 2491.
[47] J.N. Spelbrink, et al., In vivo functional analysis of the human mitochondrial DNA polymerase POLG expressed in cultured human cells, J. Biol. Chem. 275 (2000) 24818–24828.